Colliding bubble universes in eternal inflation

Nathaniel C. Thomas

Submitted to the Department of Physics

in partial fulfillment of the requirements for the degree of Bachelor of Science at the Massachusetts Institute of Technology

Signature of Author – _____

Department of Physics

May 18, 2011

Certified by — _____

Alan H. Guth

Thesis Supervisor, Department of Physics

Accepted by _____

Professor Nergis Mavalvala

Senior Thesis Coordinator, Department of Physics

Colliding bubble universes in eternal inflation

Nathaniel C. Thomas

Submitted to the Department of Physics

in partial fulfillment of the Requirements for the Degree of

BACHELOR OF SCIENCE

at the

MASSACHUSETTS INSTITUTE OF TECHNOLOGY

May 18, 2011

Abstract

We briefly summarize arguments for inflation and discuss eternal inflation. We then discuss the motion of domain walls and null shells that form in two-bubble collision processes in both the global and in-bubble FRW coordinates. Comments are made regarding possible observational signals.

Thesis Supervisor: Alan H. Guth

Title: Victor F. Weisskopf Professor of Physics

Acknowledgements

Many thanks to Professor Alan Guth for being a fantastic thesis advisor. Thanks to Dr. Ben Freivogel and Professor Raphael Bousso for helpful discussions. Thanks especially to my parents.

Contents

List of Figures

1 Introduction

With the discovery of galaxies beyond the Milky Way, astronomers increased the size of the known universe by orders of magnitude. The theory of inflation demands another radical increase in the maximum known scale: Instead of only a single universe, the theory implies the existence of a large (possibly infinite) number of other "bubble universes," born from unstable primordial energy. This collection of bubble universes is called the "multiverse." Inflationary theory requires more than simply adding more space to the universe because (due to effects from general relativity) these bubble universes are in general causally disconnected from each other; we can never see most of these universes or be seen by any scientists that may exist within them.

If we cannot send or receive signals from these regions of spacetime, we might conclude that any further investigation of them should not be labeled as scientific. However, under plausible conditions, each bubble will collide with an unbounded number of other bubbles. If ours has collided with at least one other bubble in our past, we may be able to observe astronomical evidence of the collision and therefore directly detect other bubbles.

In this thesis, we suppose that such a collision has happened and investigate its effects. We briefly discuss the theory of inflation, then consider the outcome of collisions between different types of bubbles, contributing calculations of some basic dynamics as seen from the interior of our bubble.

2 Inflationary Cosmology

In a homogeneous and isotropic universe, the most general metric is the Friedman-Robertson-Walker (FRW) metric

$$ds^2 = -dt^2 + a^2(t)\left[\frac{dr^2}{1-kr^2} + r^2(d\theta^2 + \sin^2\theta d\phi^2)\right]$$

where $0 \leq \theta \leq \pi$, $\phi \sim \phi + 2\pi$, $0 \leq r < \infty$, $k \in \{-1, 0, +1\}$, and $a(t)$ is called the *scale factor* [22]. Einstein's field equations imply that all experimentally detected types of matter cause the universe to decelerate, so $\ddot{a}(t) < 0$. *Inflation* refers to a hypothetical period in the early universe during which the opposite occurred (that is, when $\ddot{a}(t) > 0$). For this to occur, new types of matter were proposed. The simplest type of matter that allows the universe to temporarily accelerate is a scalar field. Proposing a new type of matter is justified by how successfully and elegantly the theory of inflation explains the spectrum of primordial density perturbations and resolves the following three problems with the standard hot Big Bang account of the early universe.

2.1 Three cosmological problems

We briefly present three issues with the standard hot Big Bang model and describe how they are ameliorated by cosmic inflation.

2.1.1 Horizon problem

The horizon problem is the most severe cosmological problem solved by inflation. Without inflation, there is insufficient time for disparate parts of the universe (that is, regions that are separated by more than a few degrees

in the cosmic microwave background) to thermalize uniformly; however, we observe near uniformity in cosmic microwave background radiation temperatures (*i.e.* near isotropy). Inflation allows a period during which very large regions (in comoving coordinates) can equilibrate before the period of exponential expansion that is followed by standard Big Bang cosmology.

2.1.2 Flatness problem

The universe is currently believed to be nearly spatially flat. The Friedman equation implies that the universe was far flatter in the early universe. Without inflation, we must either argue for a symmetry or mechanism that causes the universe to be perfectly flat at the Big Bang or accept an enormously fine-tuned initial value of the curvature. Inflation is a mechanism for flattening the universe, and it explains how, from natural initial conditions, the spatial curvature could have become nearly flat in the early universe.

2.1.3 Relic problem

Many grand unified theories (GUTs) that unify the standard model gauge group $SU(3) \times SU(2) \times U(1)$ predict new particles at high energies, such as magnetic monopoles in $SU(5)$. If these theories were correct and if the hot Big Bang model held at very high energies, then we would expect to see stable GUT relic particles such as monopoles now. However, no such particles have been detected.

One solution to this problem is to assume that the absence of relic particles strongly constrains the possible GUTs. This is not the only way to reconcile these data. If a period of inflation occurred after these particles

were produced, it could dilute the densities of relic particles so that they are consistent with experimental bounds.

2.2 Microphysics of inflation

The simplest model of inflation uses a single scalar field coupled to gravity to provide both the nearly uniform energy density that causes inflation and the fluctuations to seed structure formation as the universe evolved. This field is called the *inflaton*. The simplest proposal for the inflaton is a real scalar field ϕ coupled to gravity with the following action:

$$S = \int d^4x\sqrt{-g}\left[g_{\mu\nu}\partial^\mu\phi\partial^\nu\phi - V(\phi)\right]$$

By either varying the above action or imposing relativistic energy-momentum conservation, we find that the equation of motion of the inflaton for a homogeneous and isotropic universe is

$$\ddot{\phi} + 3H\dot{\phi} + \frac{dV}{d\phi} = 0$$

where $H \equiv \dot{a}/a$ (called the *Hubble parameter*).

Cosmic inflation was proposed by Guth [14] and modified by Linde [19] and Albrecht and Steinhardt [2]. The original proposal ("old" inflation) assumed a first-order phase transition in the field caused by a quantum tunneling event through a barrier from a false vacuum local minimum to the true vacuum. While the field is sitting in the false vacuum state, the space contains a uniform energy density (*i.e.* a positive cosmological constant) and is accelerating exactly as in de Sitter spacetime, with H constant and $a(t) \sim e^{Ht}$ for $t \gg 1/H$. When it decays to the true vacuum state, a bubble

of the true vacuum is nucleated inside of a region of false vacuum. This bubble can then accelerate outward in the false vacuum. This process will be described in detail in later sections.

The modified version of inflation ("new" inflation) involves a second-order phase transition that occurs when the field rolls slowly down a gently-sloped potential, where the field is slowed to its terminal velocity by the second term in the equation of motion – the Hubble friction term. While the field is slowly rolling, the spacetime is approximately de Sitter.

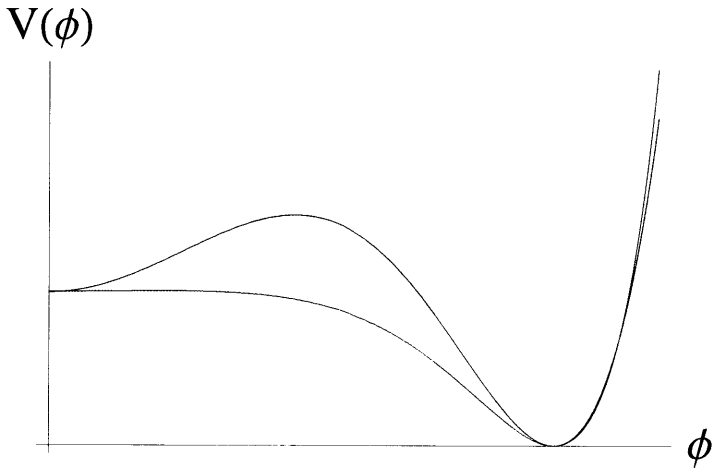

Figure 1: Potentials for the scalar field in old inflation (blue) versus new inflation (purple)

There are many more sophisticated models of inflation, but they all involve a transition between a high energy state that drives accelerated expansion to a low energy state that describes our current universe. Another simple model is hybrid inflation, where two scalar fields are considered: One drives the accelerating expansion and the other provides the primordial den-

sity perturbations. Many models are motivated by supersymmetry or string theory (see [18] for examples and references to original literature).

2.3 Generating the primordial density perturbation

The primordial density fluctuations arise from quantum fluctuations in fields that grow during inflation and become classical fluctuations. They may be calculated using semiclassical gravity methods, where the fields propagate through curved spacetime but do not backreact on the spacetime geometry. Like black holes, de Sitter space has a non-zero temperature. For a given observer, thermally distributed particles appear to be emitted from the Hubble horizon.

2.4 Comments about inflation

Inflation dilutes whatever contents the universe has accumulated before the inflationary period. While this dilution directly solves these important challenges in cosmology, it also implies that investigating the pre-inflationary epoch is challenging. Inflation can also dilute the effects of bubble collisions (described below) if the period of inflation is sufficiently long. There is a narrow window of parameters for which we may hope to observe the effects of bubble collisions through astronomical observations, and research in this area is being pursued in the hope that we are fortunate enough to inhabit that region of parameter space.

3 Eternal inflation

Inflationary models are generically eternal. This means that in nearly every model, inflation does not ever end everywhere in space – Some region of space is always accelerating roughly exponentially [15]. There are two categories of eternally inflating models: false vacuum eternal inflation (FVEI) and slow roll eternal inflation (SREI); these correspond to first- and second-order phase transitions, respectively. The mechanism of bubble nucleation in FVEI is often considered to be the Coleman-de Luccia instanton. The phenomena associated with eternal inflation become even richer when many vacua can be explored, as in the string theory landscape.

3.1 Coleman-de Luccia Instanton

The Coleman-de Luccia instanton is a type of quantum transition between two classically disconnected vacua (local minima in a potential function for a scalar field) at different energies. The higher energy is called the "false vacuum" and the lower energy is called the "true vacuum" (assuming that there are only two local minima). A field initially in the false vacuum state may tunnel quantum mechanically to the true vacuum [10]. This nucleates a bubble of the true vacuum inside of the false vacuum background. This bubble may accelerate outward in semiclassical evolution after the nucleation event. Even though the bubble takes up only a finite amount of volume in the false vacuum background, an infinite volume open universe may be contained inside of the bubble.

3.2 False vacuum eternal inflation versus slow roll eternal inflation

FVEI does not realistically model the bubble interiors because only nearly empty bubbles are created. (The deficiency of entropy inside of the bubbles is one of the reasons why old inflation was replaced.) However, FVEI provides a convenient framework in which to study bubble collisions because the thin-wall approximation can be applied. We will employ the thin-wall approximation for the remaining calculations in this thesis. This approximation treats the regions of changing scalar field as membranes with energy density and tension.

3.3 Eternal inflation and the landscape of string theory

String theory implies the existence of a vast number of vacua. These vacua include positive, negative, and zero cosmological constant solutions. For the purposes of this thesis, these will be modeled as dS, AdS, and Minkowski spaces, respectively.

The string theory landscape may help solve the cosmological constant problem – the problem of addressing why the cosmological constant is so many orders of magnitude smaller than other scales in nature such as the scales in the Standard Model or the Planck scale. A solution suggested by S. Weinberg [21] prefigured the landscape: He proposed that if there were a mechanism for generating universes with many different cosmological constants (of sufficient density), we should expect to find ourselves in a universe with a cosmological constant within a few orders of magnitude above or be-

low the one we have. Outside of this range, galaxy formation does not occur and life may not be possible. This type of reasoning is called "anthropic." Weinberg does not suggest from where this menu of universes comes. The many vacua of string theory provide the necessary diversity. There are believed to be over 10^{500} solutions to string theory, and simple models have been constructed that illustrate how varying fluxes in compact extra dimensions provide a natural way to obtain a small cosmological constant [6].

Gravitational instantons such as Coleman-de Luccia instantons provide a mechanism through which different classical minima of the string theory landscape can be populated in different bubbles. If a patch of spacetime started in a vacuum with large positive cosmological constant, a region may decay via quantum tunneling into a bubble of lower cosmological constant. Eventually, one of these bubbles is likely to be one of the vacua in the life-producing range.

4 Bubble collisions

One of the primary critiques leveled against eternal inflation is that the prediction of other bubble universes cannot be verified. However, in FVEI, each bubble will suffer an unbounded number of collisions with other bubbles [16]. (The nucleated bubbles will eventually fill all of the original de Sitter spacetime except for a set of measure zero.) If we detect these bubble collisions, we will have direct evidence for eternal inflation. It may, however, be more difficult to make any statement about the truth eternal inflation if no bubble collisions can be detected.

With the exception of the Coleman-de Luccia tunneling process, all fields are considered to behave classically.

4.1 Spacetimes with $SO(2,1)$ symmetry and the hyperbolic Birkhoff theorem

The symmetry group of de Sitter spacetime is $O(4,1)$. One way to see this is to note that de Sitter can be represented as the hyperboloid

$$-X_0^2 + \sum_{i=1}^{4} X_i^2 = H^2$$

embedded in 5D Minkowski space. When a single bubble is nucleated, this picks a preferred point in the de Sitter spacetime (or a slice of the hyperboloid in the 5D Minkowski spacetime representation), reducing the spacetime symmetry to $O(3,1)$. When two bubbles are nucleated, this picks two preferred points (or two slices of 5D Minkowski), further reducing the spacetime symmetry to $O(2,1)$. We consider the connected $SO(2,1)$ subgroup of $O(2,1)$ in this thesis.

There are three generators of the $SO(2,1)$ group. If the preferred points are spacelike separated (as is expected for most cases of bubble collisions), then two of the generators of the $SO(2,1)$ group act similarly to boosts perpendicular to the axis that connects the two preferred points and one generator acts as a rotation around this axis.

The Birkhoff theorem concludes that the metric of a spherically symmetric spacetime must be the Schwarzschild metric. Spherically symmetric spacetimes possess $SO(3)$ symmetry. (Inversion symmetry is irrelevant for our discussion, so we will consider only the connected parts of spacetime

symmetry groups.) An analogous result holds for hyperbolic spacetimes, as can be seen from analytically continuing the coordinates. Both imply that gravitational waves are excluded by the high degree of symmetry [9].

The most general metric compatible with $SO(2,1)$ symmetry is

$$d\ell^2 = -\frac{ds^2}{f(s)} + f(s)dx^2 + s^2 dH_2^2 \tag{1}$$

where

$$dH_2^2 = d\rho^2 + \sinh^2(\rho)d\phi^2$$

and

$$f(s) = 1 + \frac{\Lambda}{3}s^2 - \frac{s_0}{s}$$

where $0 < s < \infty$, $0 < \rho < \infty$, $\phi \sim \phi + 2\pi$, and $s_0 \geq 0$ [7].

4.2 Bubble collision spacetimes

We consider the most general metric compatible with $SO(2,1)$ symmetry in the following six cases: $s_0 = 0$ with $\Lambda = 0$ (Minkowski), $\Lambda > 0$ (de Sitter), $\Lambda < 0$ (anti-de Sitter), and $s_0 > 0$ with $\Lambda = 0$ (hyperbolic Schwarzschild), $\Lambda > 0$ (hyperbolic Schwarzschild-de Sitter), and $\Lambda < 0$ (hyperbolic Schwarzschild-anti-de Sitter). For each of these cases, the conformal (or Penrose-Carter diagram) is presented; in these diagrams, each point corresponds to a two-hyperboloid. To provide more information about this suppressed two-hyperboloid, Bousso wedges are placed in each region of the diagram. These V-shaped wedges are visual aids that are constructed as follows: Intersect two null geodesics in the conformal diagram. Select the directions along these geodesics along which the factor multiplying the suppressed part of the geometry in the metric (in this case, s^2 multiplying dH_2^2) is decreasing. Draw the wedge

with the legs pointing in those directions. The wedge therefore points in the direction in which the suppressed geometry is expanding [7].

4.2.1 Hyperbolic Schwarzschild

In the $\Lambda = 0$ case, the metric simplifies to

$$ds^2 = -\frac{dt^2}{h(t)} + h(t)dx^2 + t^2 dH_2^2$$

where $0 \leq t < \infty$ and $-\infty < x < \infty$ and

$$h(t) = 1 - \frac{t_0}{t}.$$

The conformal diagram is shown in Figure 2. We see that

$$R_{\mu\nu\lambda\sigma}R^{\mu\nu\lambda\sigma} = \frac{12t_0^2}{t^6}$$

so therefore there is a curvature singularity at $t = 0$ if $t_0 \neq 0$. We will only need the future diamond of the hyperbolic Schwarzschild spacetime to construct the bubble collision spacetime geometries.

4.2.2 Hyperbolic Schwarzschild-de Sitter

In the $\Lambda > 0$ case, the metric simplifies to

$$ds^2 = -\frac{dt^2}{g(t)} + g(t)dx^2 + t^2 dH_2^2$$

where $0 \leq t < \infty$ and $-\infty < x < \infty$ and

$$g(t) = 1 + \frac{\Lambda}{3}t^2 - \frac{t_0}{t}.$$

The conformal diagram is shown in Figure 3. We see that

$$R_{\mu\nu\lambda\sigma}R^{\mu\nu\lambda\sigma} = \frac{8\Lambda^2}{3} + \frac{12t_0^2}{t^6}$$

so therefore there is a curvature singularity at $t = 0$ if $t_0 \neq 0$.

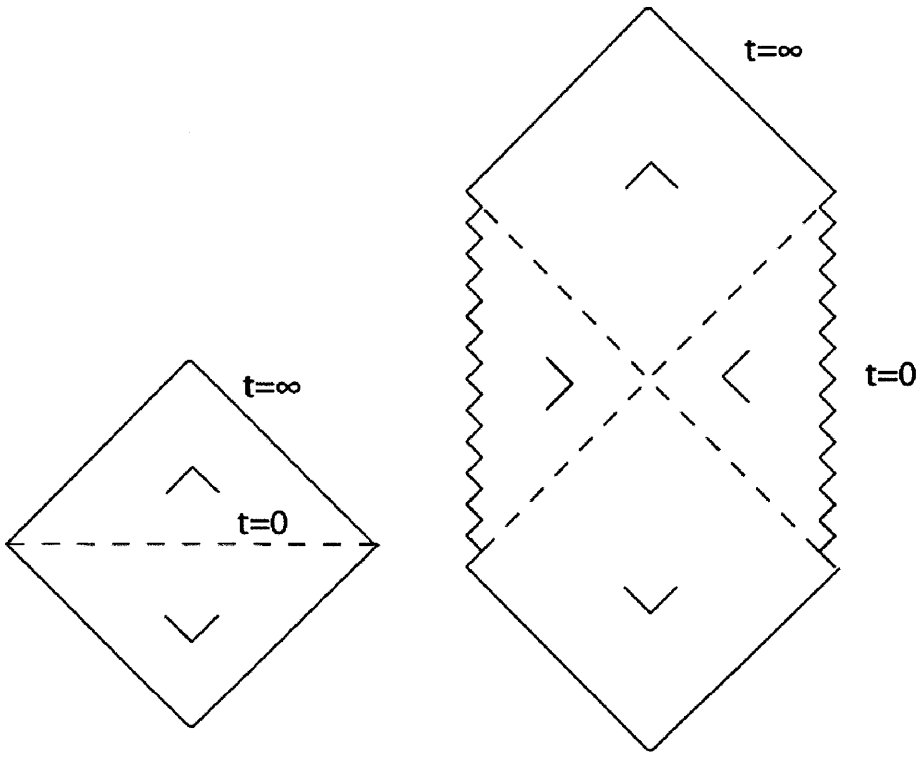

Figure 2: Conformal diagrams for Minkowski and hyperbolic Schwarzschild spacetimes (each point corresponds to a 2-hyperboloid)

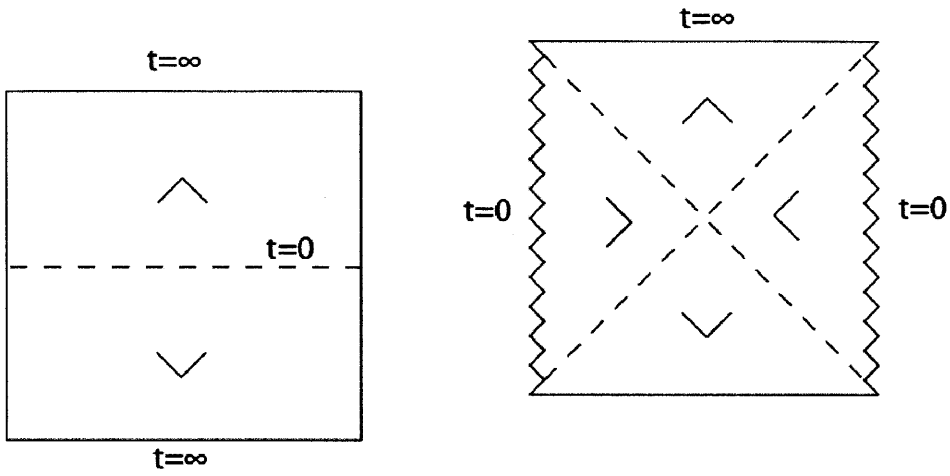

Figure 3: Conformal diagrams for dS and hyperbolic Schwarzschild dS spacetimes (each point corresponds to a 2-hyperboloid)

4.2.3 Hyperbolic Schwarzschild-anti de Sitter

In the $\Lambda > 0$ case, the metric simplifies to

$$ds^2 = -f(r)dt^2 + \frac{dr^2}{f(r)} + r^2 dH_2^2$$

where $0 \leq r < \infty$ and $-\infty < t < \infty$ and

$$f(r) = \frac{\Lambda}{3}r^2 - 1 - \frac{r_0}{r}.$$

The conformal diagram is shown in Figure 4. We see that

$$R_{\mu\nu\lambda\sigma}R^{\mu\nu\lambda\sigma} = \frac{8\Lambda^2}{3} + \frac{12r_0^2}{r^6}$$

so therefore there is a curvature singularity at $r = 0$ if $r_0 \neq 0$.

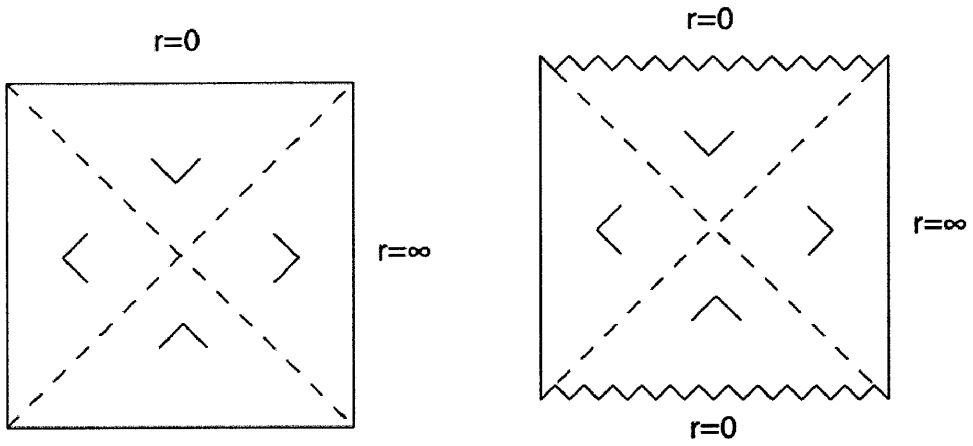

Figure 4: Conformal diagrams for AdS and hyperbolic Schwarzschild AdS spacetimes (each point corresponds to a 2-hyperboloid)

4.3 Assumptions

We make the following assumptions in the treatment of bubble collisions that follows:

- Domain wall — We assume that after two bubbles containing different vacuum states collide, a domain wall forms between them.
- Null shell of radiation — Null shells of radiation are emitted to satisfy energy-momentum conservation at the impact surface.
- Thin-wall approximation — We assume that domain walls and shells of radiation are sufficiently thin that they may be treated as membranes.
- Initially expanding — We assume that both bubbles are initially expanding after the quantum tunneling nucleation process is completed

and they begin semiclassical motion.

- Null Energy Condition

4.4 Kinematics of radiation shells and the domain wall

There will be a domain wall that separates the bubble spacetimes unless the bubbles were each in the same classical vacuum state.

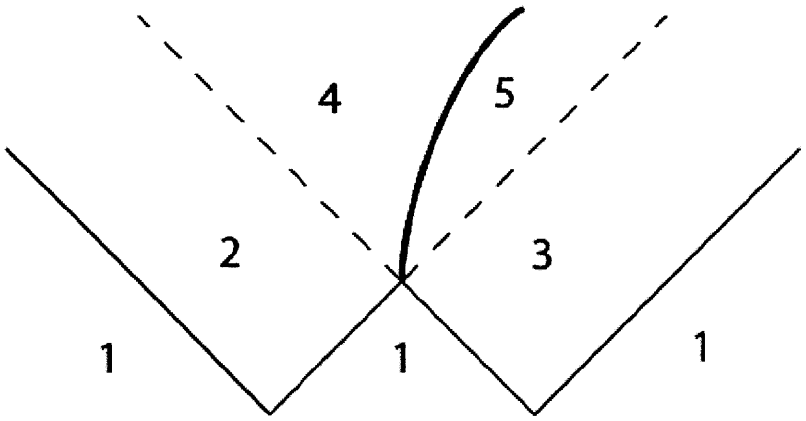

Figure 5: A spacetime diagram of a two-bubble collision in a frame in which the bubbles are nucleated simultaneously. The regions have the following properties (using the notation of the metric in Equation 4.1): (1) background metastable vacuum state ($\Lambda > 0$, $s_0 = 0$), (2) left and (3) right bubbles outside of the future lightcone of the collision ($s_0 = 0$, Λ variable), (4) left and (5) right sides of the domain wall ($s_0 \neq 0$ in general, Λ variable)

In specific simple models, null shells of radiation may be emitted in a

collision. For example in [17], the model used uses a complex scalar field in Minkowski space with the potential

$$V(\phi) = (|\phi|^2 + a)(|\phi|^2 - b)^2$$

where a and b are real constants such that $b > 2a$ (see Fig. 6). This potential has two local minima, one at $\phi = 0$ and the other at $|\phi| = b$. A bubble is formed when an instanton transition occurs between $\phi = 0$ and $|\phi| = b$. No constraints are placed on the phase of the field in the second local minimum condition; we therefore expect that different bubble interiors will have field values with different phases. When these bubbles collide, null shells of scalar radiation will be emitted from the collision. These shells propagate as a kink in the phase of the field, interpolating between the original value of the phase and the average of the two phases. (If the phase difference is nearly π, the field will be nearly antisymmetric around the plane defined by points equidistant from the nucleation points of the two bubbles. No phase waves will form, and the resulting field configuration will remain antisymmetric.) Others report similar shells of radiation in different models of bubble collisions [1] [4] [13].

It seems plausible *a priori* that bubble collisions could generate primordial black holes. However, two-bubble collisions cannot create singularities, as shown in [20]. Due to the $SO(2,1)$ symmetry, two-bubble collisions also do not create large gravitational waves according to the hyperbolic analogue of the Birkhoff theorem.

At the point of collision of the domain walls of the two bubbles, there is an inertial reference frame (according to the equivalence principle). This is equivalent to saying that no conical singularities form at the point of collision.

Consider the general collision of many sheets of matter or radiation shown

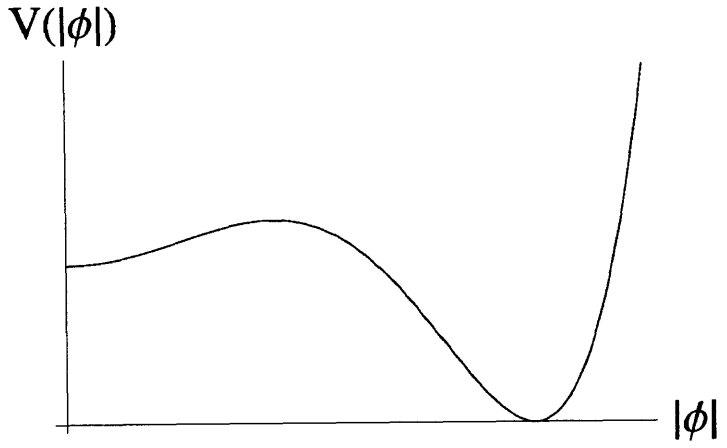

Figure 6: The shape of the double well potential considered in [17]

in Figure 7. Each (massive) sheet defines an inertial reference frame in which that sheet is at rest. The sheets of radiation can be treated by taking the limit as the velocity of massive sheets as the mass goes to zero. A boost from frame 1 to frame 2 is given by

$$\Lambda_{2,1} = \begin{pmatrix} \cosh\beta_{2,1} & \sinh\beta_{2,1} \\ \sinh\beta_{2,1} & \cosh\beta_{2,1}. \end{pmatrix}$$

The combination of two boosts results in a boost from frame 1 to frame 3:

$$\begin{aligned} \Lambda_{3,1} &= \Lambda_{3,2}\Lambda_{2,1} \\ &= \begin{pmatrix} \cosh\beta_{3,2}\cosh\beta_{2,1} + \sinh\beta_{3,2}\sinh\beta_{2,1} & \cosh\beta_{3,2}\sinh\beta_{2,1} + \sinh\beta_{3,2}\cosh\beta_{2,1} \\ \cosh\beta_{3,2}\sinh\beta_{2,1} + \sinh\beta_{3,2}\cosh\beta_{2,1} & \cosh\beta_{3,2}\cosh\beta_{2,1} + \sinh\beta_{3,2}\sinh\beta_{2,1} \end{pmatrix} \\ &= \begin{pmatrix} \cosh(\beta_{3,2}+\beta_{2,1}) & \sinh(\beta_{3,2}+\beta_{2,1}) \\ \sinh(\beta_{3,2}+\beta_{2,1}) & \cosh(\beta_{3,2}+\beta_{2,1}) \end{pmatrix} = \begin{pmatrix} \cosh\beta_{3,1} & \sinh\beta_{3,1} \\ \sinh\beta_{3,1} & \cosh\beta_{3,1} \end{pmatrix} \end{aligned}$$

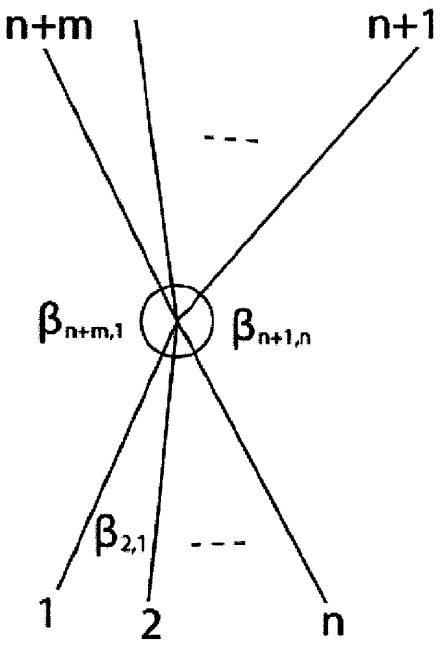

Figure 7: Figure illustrating conservation of energy-momentum at a point of collision. Time flows upward. Each line represents a sheet of matter or radiation that is entering or exiting the collision point. The βs refer to the velocity of sheet one sheet in the reference frame of another sheet.

A boost from n to $n+1$ is

$$\Lambda_{n+1,n} = \begin{pmatrix} \cosh -\beta_{n+1,n} & \sinh -\beta_{n+1,n} \\ \sinh -\beta_{n+1,n} & \cosh -\beta_{n+1,n} \end{pmatrix}$$

where $\beta_{n+1,n} > 0$ since $v_n \cdot v_{n+1} < 0$

Since the composition of all the boosts must return to the original frame if the local spacetime is flat (that is, there is no conical singularity), we obtain the following condition:

$$\Lambda_{1,n+m} \prod_{j=1}^{n+m-1} \Lambda_{j+1,j} = I_2 \Rightarrow \beta_{1,n+m} + \sum_{j=1}^{n+m-1} \beta_{j+1,j} = 0.$$

4.5 Motion of domain walls

We will now solve for the motion of the domain walls in each of these problems. To do this, we first derive the Israel junction conditions for treating surfaces in general relativity, then apply the needed conditions to domain walls in collisions between various types of bubbles (dS, AdS, Flat).

4.5.1 Israel junction conditions

We use the Gauss-Codazzi formalism to obtain the Israel junction conditions. We will use these conditions to determine the motion of the domain walls, denoted Σ, in the true and false vacuum regions. We will use Gaussian normal coordinates, where n indicates the direction normal to the domain wall. The metric in the Gaussian normal coordinates satisfies $g^{nn} = g_{nn} = 1$ and $g_{ni} = 0$. The extrinsic curvature is then given by $K_{ij} = -\Gamma^n_{ij}$. Let $S_{ij} = -\sigma g_{ij}$ be the energy-momentum tensor on the surface Σ. We make no assumptions about the functional form of σ; we will soon show that it is

constant on Σ. The components of the Einstein tensor in these coordinates are

$$\begin{aligned} G^n_n &= -\frac{1}{2}\left({}^3R + K_{ij}K^{ij} - K^2\right) \\ G^n_i &= \bar{\partial}_m K_i{}^m - \bar{\partial}_i K = 0 \\ G^i_j &= {}^3G^i{}_j - \partial_n(K^i{}_j - \delta^i_j K) - KK^i{}_j + \frac{1}{2}\delta^i_j K^2 + \frac{1}{2}\delta^i_j K_{ab}K^{ab} \end{aligned}$$

where ${}^3R$, ${}^3G^i_j$, $\bar{\partial}_m$ refer to the values of the Ricci scalar, Einstein tensor components, and partial derivatives defined intrinsically on the codimension-1 submanifold Σ [5].

Define

$$\gamma_{ij} \equiv \lim_{\epsilon\to 0}[K_{ij}(n = +\epsilon) - K_{ij}(n = -\epsilon)],$$
$$\tilde{K}_{ij} \equiv \frac{1}{2}\lim_{\epsilon\to 0}[K_{ij}(n = +\epsilon) + K_{ij}(n = -\epsilon)],$$

$\gamma \equiv g^{ij}\gamma_{ij}$, and $K \equiv g^{ij}K_{ij}$, where the $+$ and $-$ labels denote the value of the extrinsic curvature on different sides of Σ. Note that

$$\bar{\partial}_m(\gamma^m_i - \delta^m_i\gamma) = 0. \tag{2}$$

We have

$$\lim_{\epsilon\to 0}\int_{\Sigma-\epsilon\vec{n}}^{\Sigma+\epsilon\vec{n}} G_{\alpha\beta}dn = 8\pi S_{\alpha\beta} \tag{3}$$

and

$$\lim_{\epsilon\to 0}\int_{\Sigma-\epsilon\vec{n}}^{\Sigma+\epsilon\vec{n}} (\bar{\partial}_m K_i{}^m - \bar{\partial}_i K)dn = 0$$

where $\Sigma \pm \epsilon\vec{n}$ denotes evaluation on a surface moved slightly away from Σ in the normal direction. Integrating the Einstein tensor across Σ in the normal direction yields

$$\lim_{\epsilon\to 0}\int_{\Sigma-\epsilon\vec{n}}^{\Sigma+\epsilon\vec{n}} G^i{}_j dn = \lim_{\epsilon\to 0}\int_{\Sigma-\epsilon\vec{n}}^{\Sigma+\epsilon\vec{n}} ({}^3G^i{}_j - \partial_n(K^i{}_j - \delta^i_j K) - KK^i_j + \frac{1}{2}\delta^i_j K^2 + \frac{1}{2}\delta^i_j K_{ab}K^{ab})dn$$

$$
\begin{aligned}
&= -\lim_{\epsilon \to 0}(K^i_{+j} - \delta^i_j K_+ - K^i_{-j} - \delta^i_j K_-) \\
&= -\gamma^i{}_j + \delta^i_j \gamma.
\end{aligned}
$$

Combining this with Eq. 3, we find

$$\gamma_{ij} - g_{ij}\gamma = -8\pi S_{ij}.$$

This is called the first Israel junction condition.

Using junction condition and Eq. 2, we find that $\bar{\partial}_m S^{im} = 0$, so $\bar{\partial}_m(\sigma g^{im}) = 0$ and $\bar{\partial}_i \sigma = 0$. Therefore σ is constant on Σ. Contracting g_{ab} with the first Israel junction condition, we obtain

$$g_{ab}\gamma^{ab} - g_{ab}g^{ab}\gamma = 8\pi\sigma g_{ab}g^{ab}.$$

This implies that

$$\gamma = -12\pi\sigma.$$

4.5.2 Flat / flat collisions

We present a detailed discussion of a possible simple collision scenario in the case of two Minkowski bubbles colliding in an inflating background de Sitter space. This will illustrate possible domain wall dynamics. We follow [9] in this section, filling in details in the calculation at many points.

We assume that the domain walls of the two bubbles suffer an elastic collision and therefore bounce off of each other. There may be excess energy that is emitted in a null shell of scalar radiation.

We start by considering the metrics for the false vacuum region of space-time ($\Lambda > 0$ and $m_+ = 0$), the true vacuum inside of the bubbles ($\Lambda = 0$ and $m_- = 0$), the region beyond the null shells in the true vacuum ($\Lambda = 0$ and

$m_- \neq 0$ in general), and the region beyond the null shells in false vacuum ($\Lambda > 0$ and $m_+ \neq 0$):

$$d\ell^2 = -\frac{ds^2}{f_\pm(s)} + f_\pm(s)dx^2 + s^2 dH_2^2$$

where

$$f_+(s) = 1 + \frac{s^2\Lambda}{3} - \frac{2m_+}{s}$$
$$f_-(s) = 1 - \frac{2m_-}{s}.$$

We note $G^{n+}_{\ n} - G^{n-}_{\ n} = -\Lambda$, so

$$-\frac{1}{2}({}^3R + K^+_{ab}K^{ab}_+ - K^2_+) + \frac{1}{2}({}^3R + K^-_{ab}K^{ab}_- - K^2_-) = -\Lambda.$$

This conveniently eliminates the ${}^3R$. Therefore,

$$(K^+_{ab}K^{ab}_+ - K^-_{ab}K^{ab}_-) - (K^2_+ - K^2_-) = 2\Lambda. \tag{4}$$

Contracting $\tilde{K}_{ab}$ with the first Israel junction condition, we find

$$\tilde{K}_{ab}g^{ab}(8\pi\sigma) = \tilde{K}_{ab}\gamma^{ab} - \tilde{K}_{ab}g^{ab}\gamma.$$

Evaluating each of the terms in this equation gives

$$\begin{aligned}\tilde{K}_{ab}\gamma^{ab} &= \frac{1}{2}(K^+_{ab}K^{ab}_+ + K^-_{ab}K^{ab}_-) \\ \tilde{K}_{ab}g^{ab}\gamma &= \frac{1}{2}(K^+ + K^-)(K^+ - K^-) = \frac{1}{2}(K^2_+ - K^2_-).\end{aligned}$$

Combining this with Eq. 4, we find

$$\tilde{K}_{ab}g^{ab} = \frac{\Lambda}{8\pi\sigma}. \tag{5}$$

We will now use these equations to calculate the motion of the domain walls. We parametrize the domain wall motion by $\bar{x}_\pm = \bar{x}_\pm(\tau)$ and $s = s(\tau)$,

where $\dot{s} \equiv \frac{ds}{d\tau}$ and $\pm$ denotes the x position as seen from the two different regions of spacetime. The vector tangent to the domain wall is

$$u^{\alpha}_{\pm} \equiv \frac{dx^{\alpha}_{\pm}}{d\tau} = (Y_{\pm}, 0, 0, \dot{s})$$

and the normal vector is

$$n^{\pm}_{\alpha} = (-\dot{s}, 0, 0, Y_{\pm}),$$

where

$$Y_{\pm} \equiv \sqrt{\dot{s}^2 f_{\pm}^{-2} - f_{\pm}^{-1}}.$$

We will now begin to suppress the $\pm$ sub- and superscripts for notational clarity (except where $+$ or $-$ is specifically intended). Note

$$\begin{aligned} u_{\alpha}u^{\alpha} &= fY^2 - f^{-1}\dot{s}^2 = -1 \\ n_{\alpha}n^{\alpha} &= f^{-1}\dot{s}^2 - fY^2 = 1 \\ n_{\alpha}u^{\alpha} &= 0 \end{aligned}$$

Taking the covariant derivative of this first equation gives

$$\frac{D}{d\tau}(u_{\alpha}u^{\alpha}) = 2u_{\alpha}\frac{Du^{\alpha}}{d\tau} = 0,$$

which implies

$$fY\frac{D^2x}{d\tau^2} = \frac{\dot{s}}{f^2Y}\frac{D^2s}{d\tau^2}. \tag{6}$$

$$n_{\alpha}\frac{Du^{\alpha}}{d\tau} = -\dot{s}\frac{D^2x}{d\tau^2} + Y\frac{D^2s}{d\tau^2} = -\frac{1}{fY}\frac{D^2s}{d\tau^2}$$

The geodesic equation gives

$$\frac{D^2s}{d\tau^2} = \ddot{s} + \Gamma^{s}_{\mu\nu}u^{\mu}u^{\nu} = \ddot{s}\dot{s}^2\Gamma^{s}_{ss} + Y^2\Gamma^{s}_{xx}.$$

Since

$$\partial_s g_{ss} = -\frac{df^{-1}}{ds}, \partial_s g_{xx} = \frac{df}{ds}$$

and

$$\begin{aligned}\Gamma^s_{ss} &= \frac{1}{2}g^{ss}\partial_s g_{ss} = -\frac{f}{2}\frac{df^{-1}}{ds} = \frac{1}{2f}\frac{df}{ds} \\ \Gamma^s_{xx} &= -\frac{1}{2}g^{ss}\partial_s g_{xx} = \frac{f}{2}\frac{df}{ds},\end{aligned}$$

we have

$$\dot{s}^2\Gamma^s_{ss} + Y^2\Gamma^s_{xx} = -\frac{1}{2}\frac{df}{ds}$$

so therefore

$$\frac{D^2 s}{d\tau^2} = \ddot{s} - \frac{1}{2}\frac{df}{ds}.$$

Let $\vec{A} = A^i\vec{e}_i$ be an arbitrary vector in Σ. Then

$$\frac{\partial \vec{A}}{\partial \xi^j} = \frac{\partial}{\partial \xi^j}(A^i\vec{e}_i) = \vec{e}_i\nabla_j A^i + A^i\frac{\partial \vec{e}_i}{\partial \xi^j}.$$

Note that

$$\frac{\partial \vec{e}_i}{\xi^j} = -K_{ij}\vec{n}$$

since

$$\vec{n}\left(\frac{\partial \vec{e}_i}{\partial \xi^j}\right) = -K_{ij}$$

and $|\vec{n}| = 1$. Thus

$$\frac{\partial \vec{A}}{\partial \xi^j} = \vec{e}_i\nabla_j A^i - A^i K_{ij}\vec{n}$$

and

$$u^j\frac{\partial \vec{u}}{\partial \xi^j} = \vec{e}_i u^j\nabla_j u^i - u^i u^j K_{ij}\vec{n}.$$

The first term is zero because u is a geodesic on Σ. Therefore

$$\frac{Du^\alpha}{d\tau} = -u^i u^j K_{ij} n^\alpha.$$

From this, we have

$$n_\alpha \frac{Du^\alpha}{d\tau} = -u^i u^j K_{ij}, \tag{7}$$

so

$$-\frac{1}{fY}\left(\ddot{s} - \frac{1}{2}\frac{df}{ds}\right) = -u^i u^j K_{ij}.$$

Adding the + and − equations gives

$$-\frac{1}{f_+ Y_+}\left(\ddot{s} - \frac{1}{2}\frac{df_+}{ds}\right) - \frac{1}{f_- Y_-}\left(\ddot{s} - \frac{1}{2}\frac{df_-}{ds}\right) = -2u^i u^j \tilde{K}_{ij}.$$

Note that

$$\gamma_{ij} = 8\pi\sigma g_{ij} + \gamma g_{ij} = -4\pi\sigma g_{ij},$$

so

$$u^i u^j \gamma_{ij} = 4\pi\sigma u^i u^j g_{ij} = -4\pi\sigma$$

Subtracting the + and − versions of Eq. 7 gives

$$-\frac{1}{f_+ Y_+}\left(\ddot{s} - \frac{1}{2}\frac{df_+}{ds}\right) - \frac{1}{f_- Y_-}\left(\ddot{s} - \frac{1}{2}\frac{df_-}{ds}\right) = -4\pi\sigma.$$

We now compute the entries of the extrinsic curvature in the above metric:

$$\begin{aligned}
K_{ij} &= -\Gamma^n_{ij} = \frac{1}{2}\partial_n g_{ij} \\
K_{\theta\theta} &= \frac{1}{2}\partial_n g_{\theta\theta} = \frac{1}{2}\partial_n s^2 = s\partial_n s \\
K_{\phi\phi} &= \frac{1}{2}\partial_n g_{\phi\phi} = \dot{s}(\partial_n s)\sinh^2\theta + s^2 \sinh\theta \partial_n \sinh\theta = \dot{s}(\partial_n s)\sinh^2\theta \\
K_{\theta\phi} &= \frac{1}{2}\partial_n g_{\theta\phi} = 0
\end{aligned}$$

Since $\partial_n s = n^\alpha \partial_\alpha s = n^s = g^{ss} n_s = fY$ (up to sign), we have

$$\begin{aligned}
K_{\theta\theta} &= sfY = s\sqrt{\dot{s}^2 - f} \\
K_{\phi\phi} &= sf\sinh^2\theta Y = s\sinh^2\theta\sqrt{\dot{s}^2 - f}.
\end{aligned}$$

Therefore

$$\tilde{K}_{\theta\theta}g^{\theta\theta} = \tilde{K}_{\phi\phi}g^{\phi\phi} = \frac{1}{2s}(f_+Y_+ + f_-Y_-)$$

and

$$\begin{aligned} u^a u^b \tilde{K}_{ab} &= -\tilde{K}_{ab}(g^{ab} - g^{a\theta}g^{b\theta} - g^{a\phi}g^{b\phi}) \\ &= -\tilde{K}_{ab}g^{ab} + \frac{1}{s}(f_+y_+ + f_-Y_-) \\ &= -\frac{\Lambda}{8\pi\sigma} + \frac{1}{s}(f_+y_+ + f_-Y_-). \end{aligned}$$

We finally obtain

$$-\frac{1}{f_+Y_+}\left(\ddot{s} - \frac{1}{2}\frac{df_+}{ds}\right) + \frac{1}{f_-Y_-}\left(\ddot{s} - \frac{1}{2}\frac{df_-}{ds}\right) + \frac{2}{s}\sqrt{\dot{s}^2 - f_+} + \frac{2}{s}\sqrt{\dot{s}^2 - f_-} = \frac{\Lambda}{4\pi\sigma}.$$

This is the equation of motion of the domain wall in terms of $s(\tau)$. We will now simplify it and solve it in cases of interest.

Define $Z_\pm \equiv \sqrt{\dot{s}^2 - f_\pm} = -f_\pm Y_\pm$ (up to sign) and $c \equiv 2\pi\sigma$. Then

$$Z\dot{Z} = \dot{s}\left(\ddot{s} - \frac{1}{2}\frac{df}{ds}\right),$$

$$\frac{1}{\dot{s}}(\dot{Z}_+ + \dot{Z}_-) + \frac{2}{s}(Z_+ + Z_-) = \frac{\Lambda}{2c},$$

and

$$(Z_+ - Z_-) = -2cs. \tag{8}$$

Define $U \equiv Z_+ + Z_-$ and $V \equiv Z_+ - Z_-$. Then we have

$$\frac{\dot{U}}{\dot{s}} + \frac{2}{s}U = \frac{\Lambda}{2c}$$

and

$$\frac{\dot{V}}{\dot{s}} = -2c,$$

which implies that $V = -2cs + const.$ The solution for U is

$$\begin{aligned} U &= \frac{1}{2cs}(f_+ - f_-) \\ &= \frac{s\Lambda}{6c} - \frac{m_+ - m_-}{2cs^2} \\ \dot{U} &= \frac{\dot{s}\Lambda}{6c} + \frac{\dot{s}(m_+ - m_-)}{s^3 c}, \end{aligned}$$

since it is clear that

$$s\dot{U} + 2\dot{s}U = \frac{s\dot{s}\Lambda}{2c}.$$

Since $Z_\pm = \frac{1}{2}(U \pm V)$, we finally have

$$f_\pm Y_\pm = -Z_\pm = -\frac{f_+ - f_-}{4sc} \mp sc. \tag{9}$$

We examine this equation in three cases of interest:

CASE 0: $\Lambda = 0$ and $m_\pm = 0$

This case is the case of flat space in all regions of spacetime. In flat space, we have $f_+ = f_- = 1$ and $Y_\pm = \sqrt{\dot{s}^2 - 1}$. Eq. 9 then simplifies to

$$\frac{2\ddot{s}}{\sqrt{\dot{s}^2 - 1}} + \frac{4\sqrt{\dot{s}^2 - 1}}{s} = \frac{\Lambda}{4\pi\sigma} = \frac{2\epsilon^4}{\sigma},$$

where $\Lambda = 8\pi\epsilon^4$ (ϵ is the vacuum energy associated with the cosmological constant Λ). We have

$$\dot{s} = \frac{1}{\sqrt{1 - \bar{x}^2}}$$

and

$$\sqrt{\dot{s}^2 - 1} = \frac{\bar{x}'}{\sqrt{1 - \bar{x}^2}} \tag{10}$$

We have defined

$$\bar{x}' \equiv \frac{d\bar{x}}{ds},$$

so $\dot{x} = \bar{x}'\dot{s}$. Differentiating Eq. 10, we obtain

$$\ddot{s} = \frac{\bar{x}''\bar{x}'\dot{s}}{(1-\bar{x}')^{3/2}} = \frac{\bar{x}''\bar{x}'}{(1-\bar{x}')^2},$$

so

$$\frac{\bar{x}''}{(1-\bar{x}'^2)^{3/2}} + \frac{2\bar{x}'}{s\sqrt{1-\bar{x}'}} = \frac{\epsilon^4}{\sigma}$$

Rearranging this equation gives

$$\sigma s\bar{x}'' = -2\sigma\bar{x}'(1-\bar{x}'^2) + s\epsilon^4(1-\bar{x}'^2)^{3/2}$$

This agrees with [17] (after taking the opposite sign of $\bar{x}'$, which is irrelevant because the problem is symmetric around $\bar{x} = 0$).

CASE 1: $\Lambda \neq 0$, $m_\pm = 0$

This case describes expansion of bubbles before collision. Before collision, we expect the solution for the bubble walls to be physically identical to the solution obtained by assuming SO(3,1) symmetry (that is, the solution presented in [10]) because the two bubbles are not yet in contact with each other. Eq. 9 implies

$$\sqrt{\dot{s}^2 - 1} = s\left(\frac{\Lambda}{24\pi\sigma} + 2\pi\sigma\right) = \frac{s}{R}$$

where

$$R \equiv \frac{\sigma}{2\pi\sigma^2 + \Lambda/24\pi}$$

This is the same type of accelerating domain wall behavior presented in [10]. Therefore the general solution holds in two important special cases.

CASE 2: $\Lambda \neq 0$, $m_- = 0$, $m_+ \neq 0$

This case describes expansion of bubbles after the collision when no null shells are emitted. Since $m_- = 0$, we have $f_- = 1$. From Eq. 9, we have

$$f_-\dot{\bar{x}}_- = \pm\sqrt{\dot{s}^2 - 1} = 2\pi\sigma s + \frac{1}{8\pi\sigma s}\left(\frac{s^2\Lambda}{3} - \frac{2m_+}{s}\right)$$

and

$$f_+\dot{\bar{x}}_+ = \pm\sqrt{\dot{s}^2 - 1 - \frac{s^2\Lambda}{3} + \frac{2m_+}{s}} = -2\pi\sigma s + \frac{1}{8\pi\sigma s}\left(\frac{s^2\Lambda}{3} - \frac{2m_+}{s}\right).$$

$$\bar{x}' = \frac{\dot{\bar{x}}}{\sqrt{1 + \dot{\bar{x}}^2}}$$

We posit that, as measured in de Sitter space, the incoming domain wall velocity equals the outgoing velocity in subsequent collisions (which occur whenever $\bar{x} = 0$):

$$\sqrt{f_{i-1}^+\dot{s}^2 - 1}\Big|_{s=s_i^-} = \sqrt{f_i^+\dot{s}^2 - 1}\Big|_{s=s_i^+}$$

This allows us to numerically integrate the equations of motion to compute the motion of the domain walls (see Figure 8).

4.5.3 Motion of the domain wall for general collisions

For the general case, we suppose that only one domain wall is results from the collision and the rest of the energy is expelled in the null radiation shells, as in Figure 5. We summarize and quote results from [3] and [7].

On the domain wall we assume an energy-momentum tensor of the simplest form, leading to:

$$\gamma_j^i = \sigma\delta_j^i$$

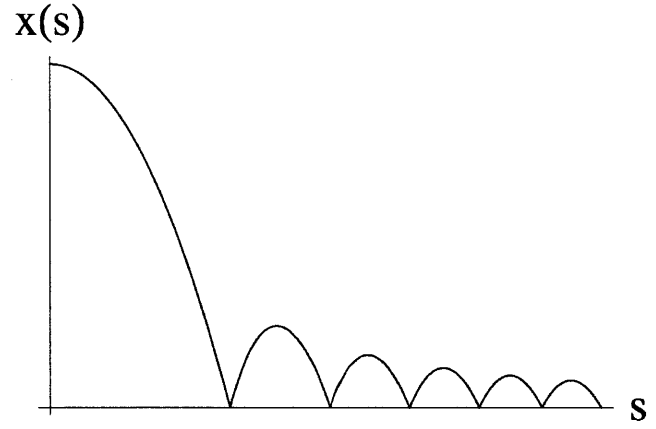

Figure 8: Motion of the domain wall separating two Minkowski bubbles after a collision (in a flat background, for simplicity)

The metric must be continuous across the domain wall according to the junction conditions, so the induced metric is

$$ds^2_{DW} = -d\tau^2 + R^2(\tau)dH_2^2$$

where $R(\tau) = t(\tau)$ or $r(\tau)$ from our previously discussed metrics. The Israel junction conditions imply

$$\zeta_L\sqrt{\dot{R}^2 + J_L(\tau)} - \zeta_R\sqrt{\dot{R}^2 + J_R(\tau)} = \sigma R$$

analogous to Equation 4.5.2, where $\zeta = \pm 1$ and $J = -h(t)$ or $-g(t)$ or $f(r)$. Solving for $\dot{R}^2$, we obtain

$$\dot{R}^2 = -V_{eff}(R) = -J_R(R) + \frac{[J_L(R) - J_R(R) - \sigma^2 R^2]^2}{4\sigma^2 R^2},$$

which reduces the problem of the domain wall motion to that of a particle in a potential. We will now state the solution of this problem for various values of the cosmological constants on either side of the domain wall.

dS / AdS or flat / AdS: For collisions between AdS and dS or flat bubbles, we have

$$\sqrt{\dot{R}^2 + f} \mp \sqrt{\dot{R}^2 - g} = \sigma R.$$

For large R, this simplifies to

$$\dot{R}^2 \approx \lambda^2 R^2$$

with

$$\lambda^2 \equiv \frac{\Lambda_{dS/flat}}{3} + \frac{1}{4\sigma^2}\left(\sigma^2 - \frac{\Lambda_{AdS} + \Lambda_{dS/flat}}{3}\right)^2$$

Using this in the junction condition gives

$$\frac{1}{2\sigma}\left|\sigma^2 + \frac{\Lambda_{AdS} + \Lambda_{dS/flat}}{3}\right| \mp \frac{1}{2\sigma}\left|\sigma^2 - \frac{\Lambda_{AdS} + \Lambda_{dS/flat}}{3}\right| = \sigma$$

We consider the following options in general for the tension σ:

- Tension greater than AdS scale – Domain wall accelerates away from dS/flat bubble (see potential in Figure 9).
- Tension equal to AdS scale – Domain wall coasts and does not accelerate (see potential in Figure 10).
- Tension less than AdS scale – Domain wall accelerates towards the dS/flat bubble. In flat / AdS collisions, this condition is impossible if the BPS bound is not violated (which will be true if supersymmetry is assumed) [3]. In dS / AdS collisions, the dS bubble is not destroyed because the domain wall can only move through part of the total expanding spacetime.

dS / flat: In dS / flat collisions, we find through similar calculations to the previous case that the domain wall accelerates away from the

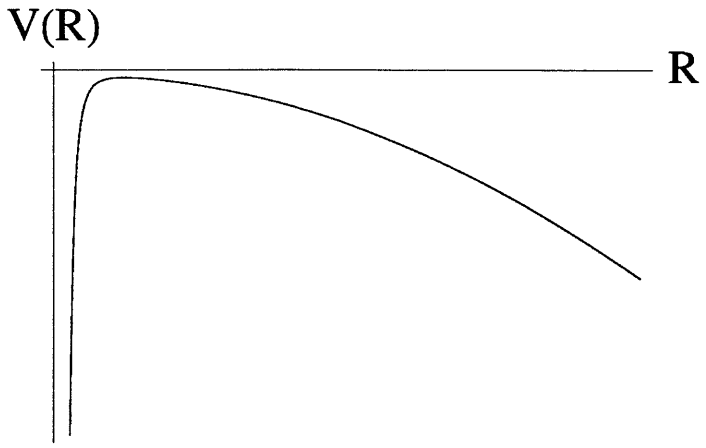

Figure 9: Form of the effective potential governing the motion of the domain wall in the non-extremal case

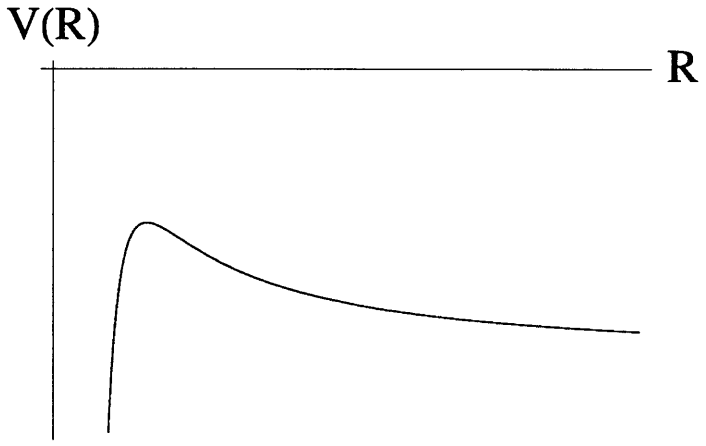

Figure 10: Form of the effective potential governing the motion of the domain wall in the BPS case

Minkowski bubble. Minkowski bubbles are therefore always safe from such collisions.

dS / dS: In a collision between two de Sitter bubbles with cosmological constants Λ_L and Λ_R, the domain wall will accelerate towards the bubble with higher cosmological constant (suppose $\Lambda_L > \Lambda_R$). This may provide an anthropic argument for a low cosmological constant if collisions are sufficiently frequent [7].

We see that observers living in bubbles with small positive cosmological constant are safe from most types of collisions.

4.5.4 Note on Raychaudhuri's Equation

In [3] and [7] it is claimed that the Null Energy Condition and the Raychauduri equation imply that "along radially directed null lines where the H_2 is decreasing it must shrink to zero size." We show this here.

The Raychaudhuri equation for a congruence of null geodesics k^μ is

$$\frac{d\theta}{d\lambda} = -\frac{\theta^2}{2} - \sigma^2 - R_{\mu\nu}k^\mu k^\nu + \omega^2$$

where $\sigma^2 = \sigma_{\rho\gamma}\sigma^{\rho\gamma}$, $\omega^2 = \omega_{\rho\gamma}\omega^{\rho\gamma}$, $\sigma_{\mu\nu} \equiv \theta_{\mu\nu} - \frac{1}{3}h_{\mu\nu}$, $\omega_{\mu\nu} \equiv h^\lambda_\mu h^\rho_\nu \nabla_{[\rho}k_{\lambda]}$, $\theta_{\mu\nu} \equiv h^\lambda_\mu h^\rho_\nu \nabla_{(\rho}k_{\lambda)}$, and $h_{\mu\nu} \equiv g_{\mu\nu} - k_\mu k_\nu$.

Using Einstein's equation, we see that

$$\begin{aligned} R_{\mu\nu}k^\mu k^\nu &= 8\pi(T_{\mu\nu} - \frac{1}{2}g_{\mu\nu}T)k^\mu k^\nu \\ &= 8\pi T_{\mu\nu}k^\mu k^\nu. \end{aligned}$$

Further, $\nabla_{[\rho}k_{\lambda]} = \partial_{[\rho}k_{\lambda]} - \Gamma^\nu_{[\lambda\rho]}k_\nu = 0$, so $\omega^2 = 0$.

If the Null Energy Condition holds, then $T_{\mu\nu}k^\mu k^\nu \geq 0$, so

$$\frac{d\theta}{d\lambda} \leq -\frac{\theta^2}{2},$$

since $\sigma^2 \geq 0$. Since $\theta = \nabla_\mu k^\mu = -2/s$, we have

$$\frac{ds}{d\lambda} \leq -1.$$

Therefore if s (the factor controlling the size of the 2-hyperboloid) is decreasing along a null geodesic, it continues to decrease to zero.

5 The view from inside

We will examine the trajectories of the null shells of scalar radiation and (asymptotically) the accelerating domain walls as they are seen from the bubble interior.

5.1 Null shells in flat background and interior

We employ three metrics for the same flat spacetime in order to determine the equation of motion for the null shells.

Flat $SO(2,1)$: $-ds^2 + dx'^2 + s^2(d\rho^2 + \sinh^2\rho d\phi^2)$

This metric is most convenient for describing the bubble collision in the collision frame.

Flat $SO(3,1)$: $-dt^2 + dx^2 + dy^2 + dz^2$

This is the standard metric for Minkowski space.

FRW in open slicing: $-d\tau^2 + \tau^2(d\xi^2 + \sinh^2\xi(d\theta^2 + \sin^2\theta d\phi^2))$

This is the standard FRW metric that covers the inside of the bubble in an

open slicing. We will center it on one of the bubbles, so the coordinates are off-center in the above $SO(2,1)$ coordinates by a distance b in the x direction.

The way to convert between the coordinates corresponding to the above metrics is as follows:

$$\begin{aligned} s\cosh\rho = \quad t &= \tau\cosh\xi \\ x'+b = \quad x &= \tau\sinh\xi\cos\theta \\ s\sinh\rho\sin\phi = \quad y &= \tau\sinh\xi\sin\theta\sin\phi \\ s\sinh\rho\cos\phi = \quad z &= \tau\sinh\xi\sin\theta\cos\phi. \end{aligned}$$

From these equations, we obtain the following:

$$\begin{aligned} \tau^2 &= s^2-(x+b)^2 \\ \tanh^2\xi &= \frac{x'^2}{s^2}+\tanh^2\rho \\ \tan^2\theta &= \frac{s^2}{x'^2}\sinh^2\rho. \end{aligned}$$

The motion of the null shell is a simple linear equation in the $SO(2,1)$ coordinates: $x' = s - 2b$. This yields the following equations:

$$\begin{aligned} \xi(\tau,\rho) &= \tanh^{-1}\left[\sqrt{\frac{\tau^2-b^2}{\tau^2+b^2}+\tanh^2\rho}\right] \\ \tan^2\theta(\tau,\rho) &= \left(\frac{\tau^2+b^2}{\tau^2-b^2}\right)\sinh^2\rho. \end{aligned}$$

Eliminating ρ, we obtain the following relationship between ξ, τ, and θ:

$$\xi(\tau,\theta) = \tan^{-1}\left(\sqrt{\frac{\frac{\tau^2-b^2}{\tau^2+b^2}\tan^2\theta}{1+\frac{\tau^2-b^2}{\tau^2+b^2}\tan^2\theta}+\frac{\tau^2-b^2}{\tau^2+b^2}}\right).$$

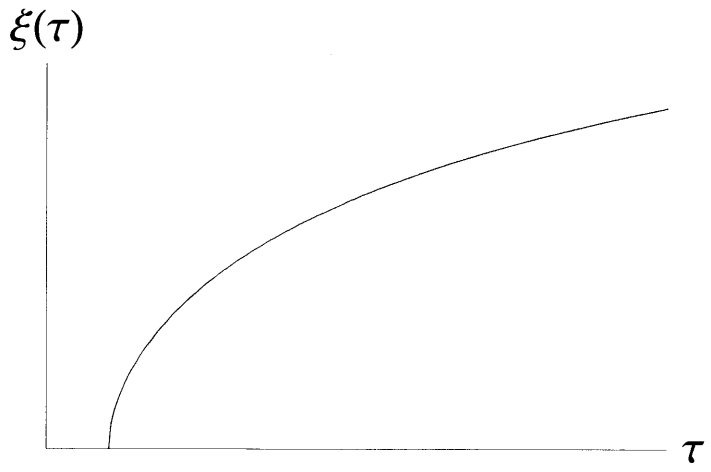

Figure 11: Sketch of null shell radius dependence on τ as seen from inside the bubble for $\theta = 0$ in a flat background and bubble interior.

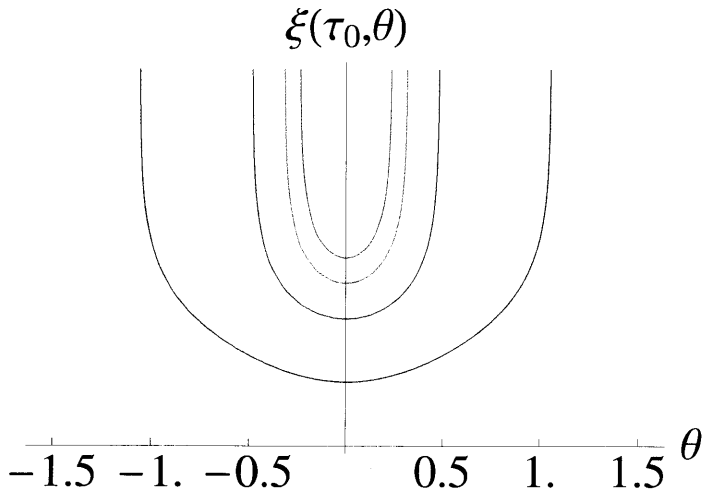

Figure 12: Sketch of null shell radius dependence on θ as seen from inside the bubble for varying τ (τ is smallest for the blue curve and increases on higher curves) in a flat background and bubble interior.

5.2 Null radiation shell in de Sitter bubbles

We will consider the motion of the null shells in the limit where $t_0 \ll t_c$, where t_c is the coordinate at which the collision occurred. This implies that to good approximation we can treat the spacetime on both sides of the null shell as flat. We will employ two metrics in this section as we used them in the previous section:

de Sitter $SO(2,1)$ metric:

$$d\ell^2 = -\frac{dt^2}{1+t^2/l^2} + \left(1+\frac{t^2}{l^2}\right)dx^2 + t^2(d\rho^2 + \sinh^2\rho d\phi^2)$$

where $x \sim x + \pi l$, $0 \leq \rho < \infty$, $0 \leq \phi < 2\pi$. (We will from here on use units for t such that $l = 1$.)

de Sitter FRW metric in open slicing:

$$d\ell^2 = -d\tau^2 + \sinh^2\tau(d\xi^2 + \sinh^2\xi(d\theta^2\sin^2\theta d\phi^2))$$

where $0 \leq \xi < \infty$, $-\pi \leq \theta < \pi$.

The equations connecting the two different sets of coordinates are [8]

$$\cosh\tau = \sqrt{1+t^2}\cos x$$
$$\sinh\tau\sinh\xi\cos\theta = \sqrt{1+t^2}\sin x$$
$$\sinh\tau\cosh\xi = t\cosh\rho$$
$$\sinh\tau\sinh\xi\sin\theta = t\sinh\rho.$$

It is clear from the above metric that null geodesics in $SO(2,1)$ obey

$$\frac{dx}{dt} = \frac{1}{1+t^2},$$

so

$$x(t) = \tan^{-1}t + 2\tan^{-1}d$$

for some constant of integration d. Let $x_0 \equiv 2\tan^{-1} d$.

We have

$$\tan x = \tanh\tau \sinh\xi \cos\theta$$

and

$$t^2 = \sinh^2\tau(\cosh^2\xi - \sinh^2\xi \sin^2\theta)$$

so

$$\tan^{-1}[\tanh\tau \sinh\xi \cos\theta] = \tan^{-1}[\sinh\tau\sqrt{\cosh^2\xi - \sinh^2\xi \sin^2\theta}] + x_0.$$

For $\tau \to \infty$ and $\theta = 0$, $\tan^{-1}(\sinh\xi) = \tan^{-1}(-\frac{1}{2}e^\tau \cosh\xi) + x_0$, where we have taken the negative square root of $\cosh^2\xi$. The value of ξ at $\theta = 0$ as $\tau \to \infty$ is

$$\xi(\tau \to \infty, \theta = 0) = \sinh^{-1}\left[\frac{1}{\tan x_0}\right].$$

This is the expected behavior of null geodesics in de Sitter space: They asymptotically approach a finite coordinate distance from any given point.

6 Observational Signatures

The $SO(2,1)$ symmetry implies that if we could observe the effects of a bubble collision, we would see them affecting a region contained inside of a disk in the CMB, since the intersection of the future lightcone of the colliding bubble, the past lightcone of an observer, and the surface of last scattering is a disk. It is unclear what we should expect to see inside of this disk, but the boundary of the disk may be a sharp boundary, defined by the maximum causal influence of the collision. Photons may be reflected by the receding domain wall between the bubbles. They would receive a red- or blue-shift

from this encounter. Another signal is that pure E-mode polarization is expected to be generated from the collision, centered around the collision [11].

7 Conclusions

7.1 Status of Observations

One group has recently presented results of an analysis that identified four candidate collision sites in WMAP data [12]. Data from the Planck satellite, especially polarization data, will be helpful in confirming these candidates or eliminating them.

Bubble collisions may have observable effects on large-scale structure. High-redshift galaxy surveys may provide evidence for bubble collisions that could be corroborated with evidence in the CMB.

7.2 Future Directions

One goal is to calculate the modified primordial density perturbation from the collision of two bubbles in the same classical vacuum. This is the simplest possible collision scenario. No domain wall would form, and only the null shells and slight deviations from isotropy would be detectable in the primordial density perturbation. This may yield a model-independent prediction of the modifications to the fluctuations that we expect to see inside of the aforementioned disks on the sky.

If we find compelling evidence that bubbles have collided with our uni-

verse, this will provide direct confirmation of eternal inflation and may provide information about the existence and nature of the string theory landscape. However, if collisions are not detected, it may be possible to use this information to constrain pictures of eternal inflation or the landscape. Such inferences may rely upon choosing an appropriate measure for calculating probabilities of events in the multiverse (a challenging problem), so there may be much work remaining on this approach.

References

[1] A. Aguirre, M. C. Johnson, and M. Tysanner. Surviving the crash: assessing the aftermath of cosmic bubble collisions. *Phys. Rev. D*, 79(12):123514, 2009.

[2] Andreas Albrecht and Paul J. Steinhardt. Cosmology for grand unified theories with radiatively induced symmetry breaking. *Phys. Rev. Lett.*, 48(17):1220–1223, Apr 1982.

[3] S. Shenker B. Freivogel, G. Horowitz. Colliding with a crunching bubble. *Phys. Rev. D*, 21:3305–3315, 1980.

[4] Jose J. Blanco-Pillado, Martin Bucher, Sima Ghassemi, and Frederic Glanois. When do colliding bubbles produce an expanding universe? *Phys. Rev. D*, 69(10):103515, May 2004.

[5] S. K. Blau, E. I. Guendelman, and A. H. Guth. Dynamics of false-vacuum bubbles. *Phys. Rev. D*, 35(6):1747–1766, 1987.

[6] Raphael Bousso and Joseph Polchinski. Quantization of four-form fluxes and dynamical neutralization of the cosmological constant. *JHEP*, 06:006, 2000.

[7] S. Chang, M. Kleban, and T. S. Levi. When worlds collide. *J. Cosmol. Astropart. Phys.*, 2008(4):034, 2008.

[8] S. Chang, M. Kleban, and T. S. Levi. Watching worlds collide: effects on the cmb from cosmological bubble collisions. *J. Cosmol. Astropart. Phys.*, 2009(4):025, 2009.

[9] W. Z. Chao. Gravitational effects in bubble collisions. *Phys. Rev. D*, 28(8):1898–1906, 1983.

[10] S. Coleman and F. de Luccia. Gravitational effects on and of vacuum decay. *Phys. Rev. D*, 21:3305–3315, 1980.

[11] Bartomiej Czech, Matthew Kleban, Klaus Larjo, Thomas S. Levi, and Kris Sigurdson. Polarizing bubble collisions. *Journal of Cosmology and Astroparticle Physics*, 2010(12):023, 2010.

[12] Stephen M. Feeney, Matthew C. Johnson, Daniel J. Mortlock, and Hiranya V. Peiris. First observational tests of eternal inflation, 2010.

[13] John T. Giblin, Lam Hui, Eugene A. Lim, and I-Sheng Yang. How to run through walls: Dynamics of bubble and soliton collisions. *Phys. Rev. D*, 82(4):045019, Aug 2010.

[14] Alan H. Guth. Inflationary universe: A possible solution to the horizon and flatness problems. *Phys. Rev. D*, 23(2):347–356, Jan 1981.

[15] Alan H. Guth. Eternal inflation and its implications. *J. Phys.*, A40:6811–6826, 2007.

[16] Alan H. Guth and Erick J. Weinberg. Could the universe have recovered from a slow first-order phase transition? *Nuclear Physics B*, 212(2):321 – 364, 1983.

[17] S. Hawking, I. G. Moss, and J. M. Stewart. Bubble collisions in the very early universe. *Phys. Rev. D*, 26(10):2681–2693, 1982.

[18] Andrew R. Liddle and David H. Lyth. *The Primordial Density Perturbation: Cosmology, Inflation and the Origin of Structure.* Cambridge University Press, first edition, 2009.

[19] Andrei D. Linde. A New Inflationary Universe Scenario: A Possible Solution of the Horizon, Flatness, Homogeneity, Isotropy and Primordial Monopole Problems. *Phys. Lett. B*, 108:389–393, 1982.

[20] I. G. Moss. Singularity formation from colliding bubbles. *Phys. Rev. D*, 50(2):676–681, 1994.

[21] Steven Weinberg. The cosmological constant problem. *Rev. Mod. Phys.*, 61(1):1–23, Jan 1989.

[22] Steven Weinberg. *Cosmology.* Oxford University Press, first edition, 2008.